

Spin-Order Driven Fermi Surface Reconstruction Revealed by Quantum Oscillations in an Underdoped High T_c Superconductor

Suchitra E. Sebastian,^{1,*} N. Harrison,^{2,†} C. H Mielke,² Ruixing Liang,^{3,4} D. A. Bonn,^{3,4} W. N. Hardy,^{3,4} and G. G. Lonzarich¹

¹*Cavendish Laboratory, Cambridge University, JJ Thomson Avenue, Cambridge CB3 0HE, United Kingdom*

²*National High Magnetic Field Laboratory, LANL, Los Alamos, New Mexico 87545, USA*

³*Department of Physics and Astronomy, University of British Columbia, Vancouver V6T 1Z4, Canada*

⁴*Canadian Institute for Advanced Research, Toronto M5G 1Z8, Canada*

(Received 17 October 2009; published 18 December 2009)

We use quantum oscillation measurements to distinguish between spin and orbital components of the lowest energy quasiparticle excitations in $\text{YBa}_2\text{Cu}_3\text{O}_{6.54}$, each of which couple differently to a magnetic field. Our measurements reveal the phase of the observed quantum oscillations to remain uninverted over a wide angular range, indicating that the twofold spin degeneracy of the Landau levels is virtually unaltered by the magnetic field. The inferred suppression of the spin degrees of freedom indicates a spin-density wave is responsible for creation of the small Fermi surface pockets in underdoped $\text{YBa}_2\text{Cu}_3\text{O}_{6+x}$ —further suggesting that excitations of this phase are important contributors to the unconventional superconducting pairing mechanism.

DOI: 10.1103/PhysRevLett.103.256405

PACS numbers: 71.45.Lr, 71.18.+y, 71.20.Ps

Potential mechanisms of high- T_c superconductivity may be elucidated by identifying precursory competing phases, the low energy excitations of which may bind Cooper pairs. The different characteristics of these contending phases must ultimately be reflected in differences in orbital, spin, or charge quantization at the Fermi surface, providing a simple means for them to be distinguished [1–5]. We use magnetic field orientation-dependent quantum oscillation measurements [6] to distinguish between spin and orbital components of the quantized Landau levels in $\text{YBa}_2\text{Cu}_3\text{O}_{6+x}$.

We present angle-dependent quantum oscillations measured in the underdoped cuprate $\text{YBa}_2\text{Cu}_3\text{O}_{6.54}$ (nominal hole doping $p \approx 0.10$ and $T_c \approx 58.7$ K) [7]. Detwinned single crystals of $\text{YBa}_2\text{Cu}_3\text{O}_{6.54}$ of dimensions $0.5 \times 0.8 \times 0.1$ mm³ are grown and prepared at the University of British Columbia [7]. The samples are attached to a coil of ~ 5 turns that forms part of a tunnel diode oscillator (TDO) circuit [8], resonating at ≈ 46 MHz when the sample is superconducting and dropping by ≈ 50 kHz on crossing over into the high magnetic field resistive state. The sample with coil is rotated *in situ*. The quantum oscillations occur by way of the Shubnikov–de Haas effect, which causes the skin depth and resonance frequency to oscillate in reciprocal magnetic field. Magnetic fields of up to 45.1 T are provided by the hybrid magnet at the National High Magnetic Field Laboratory in Tallahassee, with temperatures between ~ 0.5 and 4.2 K provided by an in-house ³He refrigerator.

We study the small Fermi surface pocket in $\text{YBa}_2\text{Cu}_3\text{O}_{6.54}$ that occupies about 2% of the unreconstructed Brillouin zone area, similar to the α pocket observed in other underdoped members of the $\text{YBa}_2\text{Cu}_3\text{O}_{6+x}$

family [9–16]. Fourier analysis of the quantum oscillations resolves a prominent frequency of $F_\alpha = 520 \pm 10$ T over the limited data range (Fig. 1)—the pocket of significantly higher frequency (β) being observed in stronger magnetic fields for this composition [17]. The α pocket cyclotron mass m_θ^* is determined at different angles θ by fitting the temperature-dependent quantum oscillation amplitude to the standard Lifshitz-Kosevich factor [6], shown in Fig. 2. The angular dependence of the quantum oscillations and effective mass associated with this pocket (Fig. 1) confirm it to be approximately cylindrical in form, typical of quasi-two-dimensional electronic structures in layered metals [18]. The anisotropy of the electronic structure of this family of materials accentuates the sensitivity of Landau quantized states to the orientation of \mathbf{H} , facilitating the use of quantum oscillations to distinguish between orbital, charge, and spin quantum numbers [6, 18, 19].

We look for interference effects in the angular dependence of the quantum oscillation amplitude measured in $\text{YBa}_2\text{Cu}_3\text{O}_{6.54}$. In the case where the spin moment is unaffected by Fermi surface reconstruction, interference between the Zeeman split spin components invariably leads to a “spin damping” factor $R_S = \cos(\phi/2)_{\text{orbital}}$ that modifies the orbitally averaged amplitude (A_θ) of the fundamental component of the quantum oscillations [6] (ϕ is the phase difference between spin-up and spin-down quantum oscillations). The standard signature of the consequent angular oscillations in (A_θ) is a series of special “spin zero” angles at which $R_S = 0$ caused by destructive interference between the two opposite spin components [6]. Importantly, the observation of such an interference effect (i.e., $R_S \neq 1$) in the angular dependence of the quantum oscillation amplitude occurs only where spin up and down

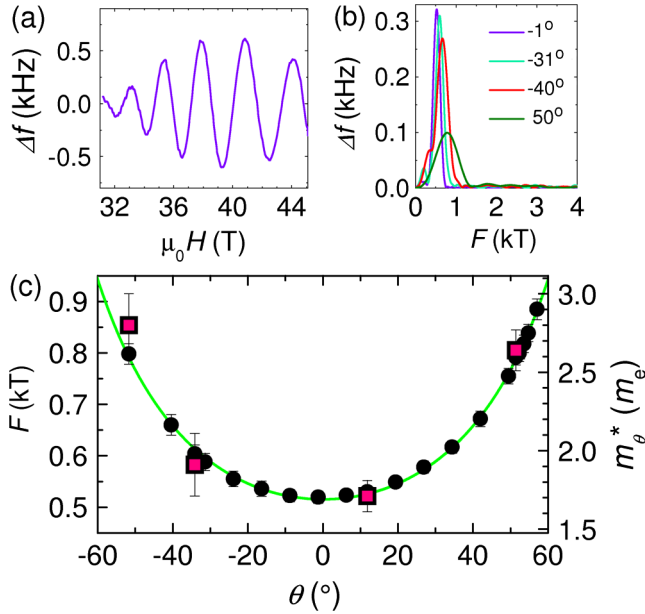


FIG. 1 (color online). Magnetic quantum oscillations in $\text{YBa}_2\text{Cu}_3\text{O}_{6.54}$. (a) The solid line shows quantum oscillations in the resonance frequency (f) of a tunnel diode oscillator (TDO) to which the sample is coupled inductively, which is proportional to the change in sample in-plane resistivity. For clarity, only the frequency shift (Δf) is shown. The nonmonotonic field dependence is likely due to a neighboring frequency of identical mass [15,16,37]. (b) Fourier analysis, in which the oscillations are multiplied by a Hann window function after background subtraction, yield a single prominent peak at all orientations θ . (c) Magnetic field orientation dependence of the quantum oscillation Fourier frequency (circles and left axis) as determined from a fast Fourier transform (FFT) of the measured oscillations. Also plotted (squares and right axis), is the experimentally determined effective mass obtained by performing fits of the temperature-dependent quantum oscillation amplitude to the Lifshitz-Kosevich expression at different angles in Fig. 2. The θ -dependent frequency and effective mass are further fit by an angular dependence $\propto 1/(\cos^2\theta + \frac{1}{\gamma}\sin^2\theta)$ (green or gray line), yielding an approximately cylindrical α Fermi surface orbit with $m_0^* = 1.7 \pm 0.1m_e$ and $F_\alpha \approx 520\text{T}$.

are individually well defined, resulting in a value of effective moment of the spin doublet $\gamma \approx 1$ (close to the free electron) associated with the relative population of spin-up and spin-down Landau levels in a magnetic field.

A striking finding from our current measurements of underdoped $\text{YBa}_2\text{Cu}_3\text{O}_{6.54}$ is that there are no spin zeros over the wide angular range accessed from -52° to 57° : on the contrary, the oscillations retain approximately the same phase over the entire range [Fig. 3(b)]. The absence of spin zeros over this wide angular range in $\text{YBa}_2\text{Cu}_3\text{O}_{6.54}$ is unsupported by a value of $\gamma \approx 1$ for the measured Fermi surface sheet (see Fig. 3). This is in contrast to the value of $\gamma \approx 1$, given by the measured Wilson ratio that appears in the expression for the enhancement in spin susceptibility $\frac{\chi_{\text{spin}}^{\text{spin}}}{\chi_{\text{electron}}^{\text{spin}}} = \gamma \frac{m^*}{m_e} \Big|_{\text{FS}}$, where γ is considered to be an average

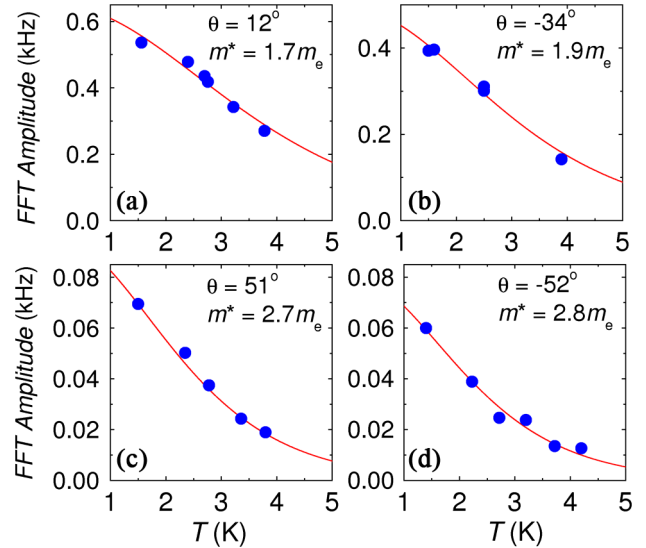


FIG. 2 (color online). Effective mass determination. The data and fits of the temperature-dependent quantum oscillation amplitude to the Lifshitz-Kosevich expression ($A = A_0X/\sinh X$, where $X = 2\pi^2 m^* k_B T / \hbar e B$ [6]) are shown together with the fitted effective masses m_θ^* and the angles θ at which each measurement was made.

over the entire Fermi surface comprising multiple sheets. Typically, $\gamma \geq 1$ in most conventional metals [6], whereas $\gamma \gg 1$ is close to a ferromagnetic instability [20]. Close to an insulating antiferromagnetic instability, γ is predicted to be of order 1 as the strength of the correlations is increased [21]. Given the proximity of the cuprates to an antiferromagnetic instability, the Wilson ratio is expected to be close to 1, and thermodynamic as well as nuclear magnetic resonance spectroscopy studies report a value of $\gamma \approx 1.1$ in $\text{YBa}_2\text{Cu}_3\text{O}_{7-x}$ [22–25]. It is worth noting that $\gamma \approx 1$ is not unique to the cuprates, but is found to be true in a wide variety of layered systems including some layered ruthenates and organic conductors [19].

Our measurements therefore indicate a suppression of the effective spin moment on the measured α Fermi surface sheet as a consequence of Fermi surface reconstruction. Moreover, we determine the expected location of spin zeros for $\text{YBa}_2\text{Cu}_3\text{O}_{6.54}$ to confirm that were they present, they would have been accessed within the angular range -52° to 57° . To first order, the ratio of the phase difference between spins (ϕ) to that between consecutive quantum oscillations (2π) is equivalent to twice the ratio of the Zeeman splitting ($\Delta\epsilon = \pm\gamma\mu_B B$)—reflecting the spin quantization [22,23] to the cyclotron energy ($\hbar\omega_c = \frac{\hbar e B_\perp}{m_0^*}$; $B_\perp = B \cos\theta$) in the orbital quantization. The location of the spin zeros is therefore given by

$$\frac{2\gamma m_0^*}{m_e \cos\theta} = 2n + 1, \quad (1)$$

where n is an integer [6]. In the case of underdoped

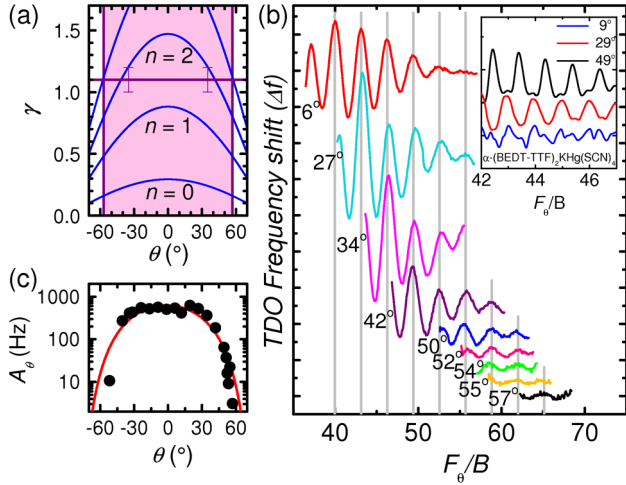


FIG. 3 (color online). Magnetic field orientation dependence of the quantum oscillations in $\text{YBa}_2\text{Cu}_3\text{O}_{6.54}$. (a) A plot of anticipated “spin zero” angles (blue or gray curves) as a function of γ determined by setting $\cos(\pi\gamma \frac{m_0^*}{m_e} \frac{B}{B_1}) = 0$, so that the angle of the n th zero is given by Eq. (1). For a Wilson ratio $\gamma = 1.1$ [24], given the experimental $m_0^* = 1.7m_e$, the first spin zero would be expected to occur at $|\theta| \approx 42^\circ$. (b) Quantum oscillations plotted versus the Landau level index $\nu = F_\theta/B$ (offset for clarity after polynomial background subtraction) shows that the relative phase of the oscillations is invariant for successive values of θ . The absence of spin zeros indicates that γ is vanishingly small (the only finite values of γ that cannot be ruled out are in the low range $0.3 < \gamma < 0.5$). The inset shows the contrasting case of a charge-density wave material $\alpha\text{-(BEDT-TTF)}_2\text{KHg(SCN)}_4$, where a “spin zero” accompanied by phase inversion of the oscillations is observed experimentally at an angle $\approx 43^\circ$ [30]. (c) Angular dependent amplitude of F_α at $B \approx 40$ T, extracted from the fast Fourier transforms of the data. The line shows the anticipated orientation-dependent amplitude according to $A_\alpha R_S \exp(-\Gamma/B \cos\theta)$ at 40 T for $R_S = 1$ (i.e., $\gamma = 0$), where the adjustable parameter Γ is a damping constant, yielding reasonable agreement with experimental amplitude.

$\text{YBa}_2\text{Cu}_3\text{O}_{6+x}$, were $\gamma = 1.1$ for the measured section of Fermi surface, we would expect the quantum oscillation amplitude to exhibit a spin zero at $|\theta| \approx 42^\circ$ in Fig. 3(a), accompanied by an inversion in the phase of quantum oscillations beyond this angle for the experimentally estimated cyclotron mass of $m_0^* = 1.7 \pm 0.1m_e$ [Figs. 1(c) and 2(a)]. The effect of spin-orbit coupling is neglected here for simplicity, since it has a relatively small effect in $\text{YBa}_2\text{Cu}_3\text{O}_{6+x}$, with a measured Landé g factor ~ 2.1 [22]—a value that is also close to the free-electron value of 2 [23].

The approximately constant phase of the quantum oscillations we observe between -52° and 57° in $\text{YBa}_2\text{Cu}_3\text{O}_{6.54}$ therefore reveals a vanishingly small value of γ in Eq. (1), corresponding to the measured small α Fermi surface pockets (inferred from Fig. 3; also indicated in the figure is a small range of very low γ that cannot be

ruled out). The absence of spin zeros is therefore inconsistent with small Fermi surface pockets arising from within the band structure (where γ close to unity [1–5,26–29]) or pockets resulting from an order parameter that couples states of like spin [see Fig. 4(b) for examples such as charge order]. An example is shown in the inset to Fig. 3(b) for the charge-density wave material $\alpha\text{-(BEDT-TTF)}_2\text{KHg(SCN)}_4$, which has very similar Fermi surface parameters (i.e., frequency, effective mass, and Wilson ratio) to $\text{YBa}_2\text{Cu}_3\text{O}_{6.54}$. As expected, a “spin zero” accompanied by phase inversion of the oscillations is observed experimentally at an angle of $\sim 43^\circ$ [30].

Our finding that the effective moment of the spin doublet is suppressed for the measured orbit (i.e., $\gamma \rightarrow 0$), has implications for the nature of ordering associated with the creation of the observed α Fermi surface sheet in underdoped $\text{YBa}_2\text{Cu}_3\text{O}_{6+x}$. For types of magnetic ordering where opposite spins couple, a suppression of the effective moment of the spin doublet can result (i.e., $\gamma \rightarrow 0$), in which case B cannot lift the Landau level spin degeneracy to leading order. The order parameter consistent with both the creation of small Fermi surface pockets and the coupling of spin-up and spin-down down states is a spin-density wave state [31]. In this case, spin is no longer well defined for the Landau quantized states, so that the effective moment of the spin doublet becomes $\gamma \approx 0$ in Eq. (1) [see Fig. 4(c)]. The layered Bechgaard salts [31,32] provide well-known examples of spin-density wave phases exhibiting such a robust twofold degeneracy of the Landau levels, where $\gamma \sim 0$ is rigorously confirmed by experiment.

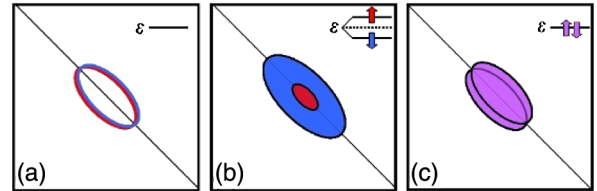


FIG. 4 (color online). Example of the effect of Zeeman splitting on Fermi surface reconstruction. We consider the simple case of a hole pocket at $(\pi/2, \pi/2)$ created by commensurate ordering with $\mathbf{Q} = (\pi, \pi)$ for illustrative purposes. (a) Schematic of a twofold degenerate holelike Fermi surface pocket in the absence of a magnetic field, intersected by a Bragg reflection plane (diagonal line). (b) Schematic showing the Zeeman splitting of the twofold degeneracy (if spin up and spin down are individually well defined so that $\gamma = 1$). The red or center shaded area denotes a spin-up Fermi surface while the blue or outer shaded area denotes a spin-down Fermi surface. (c) Schematic showing how the pocket size remains largely invariant to Zeeman splitting if the order parameter couples up and down spins (as in the case of a spin-density wave, so that $\gamma = 0$). The purple (shaded) areas show Fermi surfaces comprising spins where the effective moment has been suppressed, potentially due to spin flips at Bragg reflection. While $\mathbf{Q} = (\pi, \pi)$ is considered for this simple schematic, $\gamma \ll 1$ is expected for more general SDW wave vector scenarios [38].

In Fig. 3(c), we also compare the θ -dependent attenuation of the quantum oscillation amplitude in $\text{YBa}_2\text{Cu}_3\text{O}_{6.54}$ with that predicted for $\gamma = 0$ (assuming the exponential damping factor due to disorder scattering depends only on B_{\perp}), and find reasonable consistency.

Our present finding that $\gamma \ll 1$ for the α orbit indicates that spin ordering is associated with the creation of the α Fermi surface pocket in $\text{YBa}_2\text{Cu}_3\text{O}_{6.54}$. Additional evidence is provided by recent elastic neutron scattering measurements made on nearby $\text{YBa}_2\text{Cu}_3\text{O}_{6+x}$ sample compositions that reveal magnetic field-enhancement of spin ordering [33–35]. The current findings are therefore likely applicable to a range of hole dopings within the underdoped regime [14]. It is possible that other order parameters such as a triplet d -density wave (also referred to as “unconventional spin-density wave”) [36] could also result in the observed suppression of γ .

Our results indicate that at measured magnetic fields above the order of 30 T, the ground state associated with the measured small Fermi surface pockets in the cuprates is a spin-density wave. Since the present technique provides direct access to the lowest energy excitations [1–5], the proximity to spin ordering and its sensitivity to a magnetic field indicates the existence of soft spin excitations in $\text{YBa}_2\text{Cu}_3\text{O}_{6.54}$ and potentially other dopings in the underdoped regime of high temperature superconductors [14,33–35]. An implication is that magnetic fluctuations may play an important role in the pairing mechanism of carriers in cuprate superconductors. These observations contribute to an overarching picture of the intimate connection of spin excitations to unconventional superconducting pairing.

This work is supported by Trinity College (Cambridge University), U.S. Department of Energy, the National Science Foundation, and the state of Florida. The authors thank T. P. Murphy, G. Jones, and J. Billings for technical assistance.

*suchitra@phy.cam.ac.uk

†nharrison@lanl.gov

- [1] S. Chakravarty, R. B. Laughlin, D. K. Morr, and C. Nayak, *Phys. Rev. B* **63**, 094503 (2001).
- [2] S. A. Kivelson *et al.*, *Rev. Mod. Phys.* **75**, 1201 (2003).
- [3] P. W. Anderson *et al.*, *J. Phys. Condens. Matter* **16**, R755 (2004).
- [4] P. A. Lee, N. Nagaosa, and X. G. Wen, *Rev. Mod. Phys.* **78**, 17 (2006).
- [5] C. M. Varma, *Phys. Rev. B* **73**, 155113 (2006).
- [6] D. Schoenberg, *Magnetic Oscillations in Metals* (Cambridge University Press, Cambridge, 1984).
- [7] R. Liang, D. A. Bonn, and W. N. Hardy, *Phys. Rev. B* **73**, 180505(R) (2006).
- [8] T. Coffey *et al.*, *Rev. Sci. Instrum.* **71**, 4600 (2000).

- [9] N. Doiron-Leyraud *et al.*, *Nature (London)* **447**, 565 (2007).
- [10] D. LeBoeuf *et al.*, *Nature (London)* **450**, 533 (2007).
- [11] E. A. Yelland *et al.*, *Phys. Rev. Lett.* **100**, 047003 (2008).
- [12] A. F. Bangura *et al.*, *Phys. Rev. Lett.* **100**, 047004 (2008).
- [13] C. Jaudet *et al.*, *Phys. Rev. Lett.* **100**, 187005 (2008).
- [14] S. E. Sebastian *et al.*, *Nature (London)* **454**, 200 (2008).
- [15] A. Audouard *et al.*, *Phys. Rev. Lett.* **103**, 157003 (2009).
- [16] S. E. Sebastian *et al.* (unpublished).
- [17] S. E. Sebastian *et al.*, arXiv:0910.2359.
- [18] *The Physics of Recent Organic Superconductors and Conductors*, edited by A. Lebed (Springer-Verlag, Berlin, 2008).
- [19] R. H. McKenzie, arXiv:hep-ex/9905044.
- [20] E. Bucher *et al.*, *Phys. Rev. Lett.* **18**, 1125 (1967).
- [21] P. Fazekas, *Lecture Notes on Electron Correlation and Magnetism* (World Scientific, Singapore, 1999).
- [22] R. E. Walstedt *et al.*, *Phys. Rev. B* **45**, 8074 (1992).
- [23] Strong spin-orbit interactions combined with the coupling of the orbitals to the crystalline electric field can cause the effective g factor (and therefore γ) to become anisotropic. Such effects are readily encountered in f -electron systems but typically lead to an anisotropy of order 10% or less in the case of Cu^{2+} .
- [24] J. W. Loram *et al.*, in *Superconductivity VII: Proceedings of the 7th International Symposium on Superconductivity* (Springer-Verlag, Tokyo, 1995), Vol. 1, p. 75.
- [25] J. D. Thompson *et al.*, in *Proceedings of the 18th International Conference on Low Temperature Physics, Kyoto* [*Appl. Phys.*, Suppl. 26-3, 2041 (1987)].
- [26] A. J. Millis and M. R. Norman, *Phys. Rev. B* **76**, 220503 (R) (2007).
- [27] W.-Q. Chen, K.-Y. Yang, T. M. Rice, and F. C. Zhang, *Europhys. Lett.* **82**, 17004 (2008).
- [28] P. A. Lee, *Rep. Prog. Phys.* **71**, 012501 (2008).
- [29] I. Dimov, P. Goswami, X. Jia, and S. Chakravarty, *Phys. Rev. B* **78**, 134529 (2008).
- [30] N. Harrison *et al.*, *Phys. Rev. B* **63**, 195102 (2001).
- [31] P. M. Chaikin, *J. Phys. I (France)* **6**, 1875 (1996).
- [32] W. Kang, H. Aoki, and T. Terashima, *Synth. Met.* **103**, 2119 (1999).
- [33] C. Stock *et al.*, *Phys. Rev. B* **77**, 104513 (2008).
- [34] V. Hinkov *et al.*, *Science* **319**, 597 (2008).
- [35] D. Haug *et al.*, *Phys. Rev. Lett.* **103**, 017001 (2009).
- [36] C. Nayak, *Phys. Rev. B* **62**, 4880 (2000).
- [37] F_{α} is found to have an identical mass as the two neighboring frequencies in [16], indicating that our findings here regarding the spin splitting factor are unaltered.
- [38] For more general SDW wave vectors, $\gamma = 0$ is strictly true for a pocket whose trajectory encompasses equal areas in the first and second Brillouin zones (or that contains a symmetric mixture of spin-up and spin-down states). Should these areas be unequal, a small residual Zeeman splitting of the Landau levels can result (reflecting the inequality in areas), giving rise to a small but finite γ . A very small value of $\gamma \ll 1$ cannot be ruled out in the present study.